

Ultra-sensitive broad-dynamic range optical magnetometer with instance response to magnetic field changes

Przemysław Włodarczyk^a, Szymon Pustelny^{b,c}, Jerzy Zachorowski^b, and Marcin Lipiński^a

^a *Department of Electronics, AGH University of Science and Technology*
Mickiewicza 30, 30-059 Krakow, Poland

^b *Institute of Physics, Jagiellonian University*
Reymonta 4, 30-059 Krakow, Poland
E-mail: pustelny@uj.edu.pl

^c *Department of Physics, University of California at Berkeley*
Berkeley, California 94720-7300, USA

ABSTRACT: We investigate one of the most sensitive devices for measuring magnetic fields, the, so-called, AMOR magnetometer. The device exploits a specific nonlinear optical phenomenon (amplitude-modulated nonlinear magneto-optical rotation) for ultra-precise magnetic field detection. It allows measuring the field with a sensitivity of 10^{-14} T/Hz^{1/2} within a dynamic range of 10^{-4} T. Such high sensitivity and the dynamic range covering the Earth magnetic field are desired in context of many practical application of the device. By elaborating the electronic model of the magnetometer we study its different characteristics in various arrangements. It allows us to optimize the device regarding different requirements, e.g., technical simplicity, data processing, etc. It is shown that the device may be automated operating it in the self-oscillation mode. Particularly, we show that the magnetometer instantly responses to the magnetic field change. Our numerical analyses are confirmed with experimental results obtained in one of the arrangements.

KEYWORDS: Magnetometry; Magneto-optical rotation; Numerical simulations of electronic circuits.

| | |
|--|-----------|
| 1. Introduction | 2 |
| 2. Optical magnetometer based on amplitude-modulated nonlinear magneto-optical rotation | 3 |
| 2.1 Real system | 3 |
| 2.2 Electronic equivalent | 6 |
| 3. Simulations | 6 |
| 3.1 General information | 6 |
| 3.2 Model verification | 7 |
| 3.3 Different detection scheme in self-oscillation mode | 8 |
| 3.3.1 Modulated pump, unmodulated probe, balanced polarimeter | 8 |
| 3.3.2 Modulated pump, unmodulated probe, (nearly) crossed analyzer | 9 |
| 3.3.3 Single-beam arrangement with balanced polarimeter | 10 |
| 3.3.4 Single beam with (nearly) crossed analyzer | 11 |
| 4. Experimental results | 13 |
| 5. Conclusions | 14 |

1. Introduction

Magnetocardiography is one of the most promising future medical diagnostic techniques. The method is based on detection and analysis of the magnetic field generated by human heart [1]. Detection of the field provides information about distribution and flow of biocurrents in the muscle and hence gains information about heart's condition. An important advantage of the method over traditionally used electrocardiography is a possibility of acquiring information about the internal parts of the heart (heart outer layers are electrically shielding interior of the muscle) since the biocurrent-generated magnetic fields easily penetrate through the human body.

A particular challenge of magnetocardiography is the strength of a magnetic field generated by a human heart. The peak value of this field measured just above the man's chest is roughly a million times weaker than the Earth magnetic field [1]. It implies application of ultra-sensitive magnetometric technique and often shielding or compensation of external, uncontrollable fields, such as the Earth magnetic field, field from moving objects (cars, elevators, etc.), and fields generated by AC lines. Such high sensitivity may, for example, be obtained with optical magnetometers, i.e., the devices that utilize a magnetic-field dependent change of a specific property (e.g. intensity, polarization) of light traversing the medium subjected to the magnetic field (see Ref. [2] and references therein).

Recently, magnetic fields generated by a human heart were measured and mapped using the technique exploiting amplitude modulated nonlinear magneto-optical rotation (AMOR) in partially shielded environment [3]. Due to its high sensitivity and broad dynamic range the

method limits the necessity of external-field shielding, which in addition to low cost and almost no maintenance make the technique very attractive for a number of applications including magnetocardiography.

The AMOR magnetometer has a few experimental realizations. The most differences are related to light-detection schemes which results in different time dependence of detected optical signal. In this paper we investigate four of the AMOR-magnetometer arrangements by constructing electronic models. It allows us to analyze advantages and disadvantages of all arrangements. In particular we investigate a possibility of automated operation of the device in the, so-called, self-oscillating mode. This studies show that such mode allows one to track magnetic-field changes with instant response to the change. The electronic models also enable to optimize the electronics for the detection schemes which eventually led to demonstration of the AMOR-magnetometer operation in one of the arrangements.

2. Optical magnetometer based on amplitude-modulated nonlinear magneto-optical rotation

2.1 Real system

Resonant interaction of intense, linearly polarized light with a medium may lead to generation of optical anisotropy [4]. Such anisotropy is present during the interaction and fades out after the light is off within very short time (on the order of ps or shorter). However, in some media, e.g., dilute gases enclosed in specially prepared containers, the anisotropy lifetime after the light is off may be as long as a second. It enables to observe rotation of the anisotropy axis, via detection of rotation of light polarization plane, which results from interaction of atoms or molecules constituting the medium with external magnetic fields they are subjected to. The precession frequency of the anisotropy is determined by the magnetic field (the Larmor frequency Ω_L) and hence it can be used as a measure of the field. Such optical technique may be applied to detect weak magnetic fields (with CW light) or much stronger fields, e.g., comparable with the Earth magnetic field (with modulated light) [5]. In the latter case the anisotropy precessing around the magnetic field is generated when resonant condition between the light-modulation frequency Ω_m and the Larmor frequency are fulfilled

$$\Omega_m = 2\Omega_L = kB,$$

where k is the material constant and B is the strength of the magnetic field. The effect is known as amplitude-modulated nonlinear magneto-optical rotation (AMOR) and it can be used to measure magnetic field in broad dynamic range (relative sensitivity of 10^{-10}).

Block diagrams of the magnetometer based on amplitude-modulated nonlinear magneto-optical rotation (AMOR) is shown in Fig. 1. The figure presents two modes of magnetometer operation: (a) the passive mode, where light modulation is induced by an external oscillator [6], and (b) the self-oscillating mode, where the output of the magnetometer is used as the modulation input.

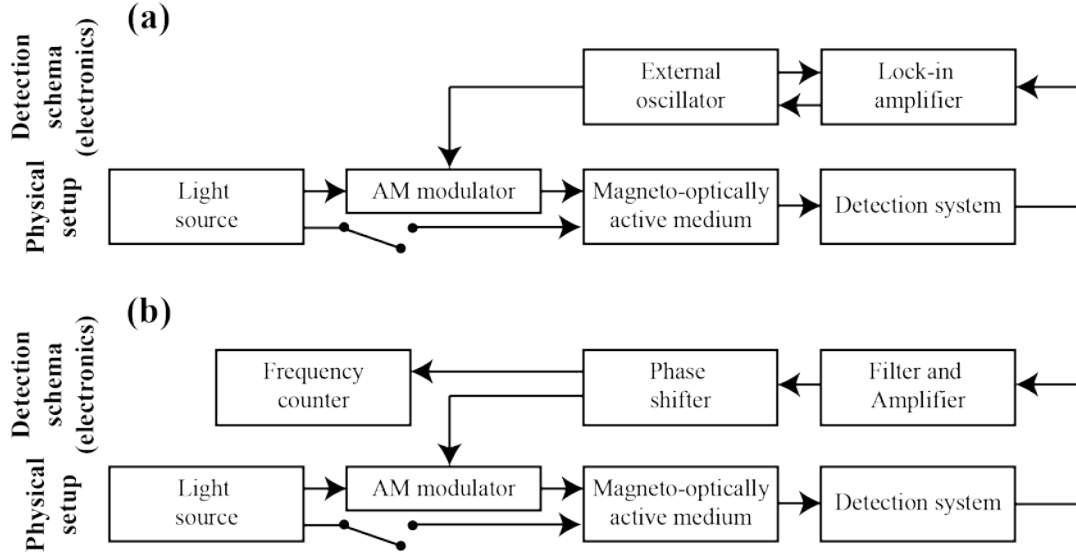


Figure 1. Block diagram of AMOR magnetometer. (a) Passive mode. (b) Self-oscillation mode.

There are four different arrangements of the AMOR magnetometer. The first two arrangements exploit the, so-called, balanced polarimetry at the detection stage. In this scenario the detected signal is proportional to the angle of polarization rotation and incident light intensity. Since AMOR magnetometers may be operated using a single light beam, e.g., the same beam is used for generation and detection of anisotropy, or with two independent light beam where additional unmodulated light is used to detect the anisotropy, there are two different characteristics of the output electric signal (convoluted or unaffected with the modulation). The other two arrangements exploit the, so-called, nearly crossed polarizer technique where just a single photodiode situated by the polarizer rotated by $\sim 90^\circ$ with respect to the incident light polarization is used. In the cases the detected signal is proportional to the square of the polarization-rotation angle and intensity of light.

Table 1 summarizes all four arrangements along with the mathematical formulas describing the output signals measured in each of them. The formulas are derived using the Malus law for sinusoidally modulated light¹. The first two cases correspond to the pump-probe arrangement (two beams) while the other two to single-beam arrangement. The first and third row formulas show relations for balanced-polarimeter detection scheme, while the second and fourth to the nearly perfectly crossed polarizers. The last column shows the corresponding formulas used in our simulations.

In order to track the changes of the magnetic field using AMOR the resonance conditions need to be fulfilled (see above). It can be realized in the, so-called, passive mode in which external oscillator modifies the modulation frequency using the feedback loop in order to maximize the AMOR-signal amplitude (Fig. 1a) [6]. This solution has an advantage of a high signal-to-noise ratio (SNR) due to the application of phase-sensitive detection, but has also a significant drawback. It tracks the magnetic-field changes iteratively and each change of the

¹For small rotation angles typically on the order of a few degrees $\sin x \approx x$, which is used in Table 1.

field is followed by a number of steps in which the modulation frequency is modified. Such approach is time consuming, particularly, when larger integration constants (better SNR) are used and/or magnetic-field changes exceed the width of the AMOR resonance (usually about 10^{-8} T). Another approach is the so-called self-oscillation mode and it bases on the seminal work of Bloom (Fig. 1b) [7]. In this approach filtered, amplified, and phase shifted output AMOR signal is used to modulate the pumping light. In such a case all magnetic-field changes leads to modification of the modulation frequency so that the resonance condition is instantly fulfilled.

Table 1. Different detection schemes for AMOR manngnetometry. Third column provides mathematical formulas describing detected optical signals. For simplicity, it was assumed that the pump-light intensity is sinusoidally modulated. Last column shows electric signals recorded in electronic equivalent of each arrangement. A is the amplitude of the polarization rotation, Θ is the uncrossing angle, and I_0 is the probe beam intensity.

| Beams arrangement | Detection arrangement | Mathematical formula describing recorded signal | Function characterizing the source B1 in Fig. 2 |
|-------------------------|---------------------------|--|--|
| Pump-probe Arrangement | Balanced polarimeter | $I_0 A \sin \Omega_m t$ | $A * V(\text{atoms})$ |
| | (Nearly) crossed analyzer | $I_0 (A \sin \Omega_m t + \Theta)^2$ | $[A * V(\text{atoms}) + \Theta]^2$ |
| Single-beam Arrangement | Balanced polarimeter | $I_0 / 2 (1 + \sin \Omega_m t) A \sin \Omega_m t$ | $A * V(\text{atoms}) * V(\text{laser})$ |
| | (Nearly) crossed analyzer | $I_0 / 2 (1 + \sin \Omega_m t) (A \sin \Omega_m t + \Theta)^2$ | $[A * V(\text{atoms}) + \Theta]^2 * V(\text{laser})$ |

2.2 Electronic equivalent

By its nature, AMOR remains a driven damped harmonic oscillator, where “the length of a pendulum” and, correspondingly, the oscillation period is determined by the magnetic field. Thus the non-electronic part of the AMOR magnetometer has a simple electronic equivalent, which may be easily simulated with electronic circuit simulation software such as Spice. It allows one to investigate different scenarios and elaborate the electronic circuits best suited for the particular solution.

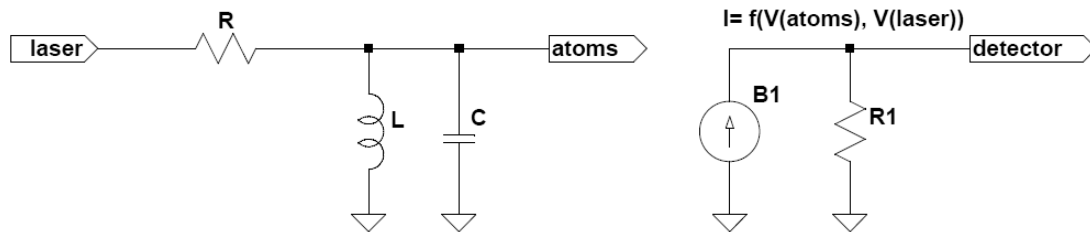


Figure 2. Electronic equivalent of the “Physical setup” used in simulations of the magnetic field.

The first part of the model is a RLC circuit shown in the left-handed side of Fig. 2. The circuit models generation of the optical anisotropy in gas with a strong resonance character. In order to reproduce the parameters of the AMOR signal measured in rubidium vapor in the Earth magnetic field of $\sim 50 \mu\text{T}$ (operation in magnetically unshielded environment), the resonance frequency of the circuit was set to 700 kHz by appropriate choice of the values of the electronic elements. The width of the resonance ($\sim 30 \text{ Hz}$) and hence the Q factor of the circuit was adjusted by a careful set of the value of resistor R.

The second part of Fig. 2 presents electronic circuit modeling the detection system in a real setup. It consists of the current source B1 and resistor R1. The effect of atoms on the properties of the light beam and hence the electric signals recorded at the detection stage is represented by a nonlinear function $f(V(\text{atoms}), V(\text{laser}))$. The function takes different forms depending on a particular configuration of the experimental setup (see Tab. 1) which enabled us to investigate different scenarios for AMOR magnetometry.

3. Simulations

3.1 General information

The electronic circuits were simulated in the time domain with LTspice IV by Linear Technology. In each of the considered cases, the maximum time-step size was 3 ns. Such a small step was chosen to minimize the error of the transient analysis, which becomes significant when analyzing resonant circuits with very high Q factor.

Since the main purpose of the analysis was to investigate the possibility of operating AMOR magnetometer in the self-oscillating mode (see Fig. 1), the absolute amplitude values of the signals were not important. It allows us to set the amplitude of the oscillation of polarization rotation A equal to 1. The decrossing angle Θ is a parameter which can be freely chosen in the experimental setup. We have performed the simulations for a broad range of the Θ/A ratios between 0.001 and 1000 and found that self-oscillation requires only proper tuning of amplification. We present therefore the results for the simplest case of $\Theta = A = 1$.

3.2 Model verification

In order to verify the existing model and compare the AMOR experimental signals recorded in the passive-mode arrangement (Fig. 1) with the ones obtained in our simulations the electronic circuit was designed (Fig. 3). The circuit corresponds to the AMOR experiment in which modulated pump and unmodulated probe are used (pump-probe arrangement) and the signal is measured using balanced polarimeter (first row in Table 1). The behavior of the circuit was simulated by sweeping the frequency of the quadrature generator realized by ramping the V_{ramp} voltage. Components B2, R2, C2, and B3, R3, C3 forms synchronous detection circuit and represent the lock-in amplifier used in the experiment. Voltages at its outputs correspond to the in-phase and quadrature components of the signal measured in the experiment. Capacitors C_i determine time constants of integration. Capacitance values were set in order to obtain the tradeoff between accuracy and simulation time. The 1-V DC voltage source between the

generator and the resonant circuit assures that voltage $V(\text{laser})$ corresponding to light intensity may not become negative.

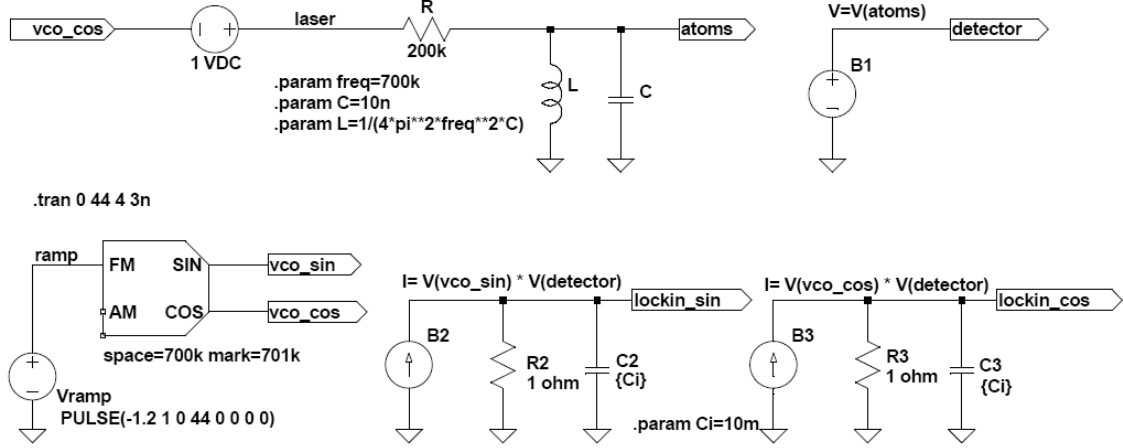


Figure 3. Circuit diagram and simulation parameters of electronic equivalent of the AMOR setup with balanced polarimeter in pump-probe arrangement (upper circuits) where optical signal is detected using lock-in amplifier (lower circuits).

Figure 4(a) shows the results obtained in the simulation. The amplitude R was calculated from in-phase x (sin) and quadrature y (cos) components of the signal with the formula $R = \sqrt{x^2 + y^2}$. As shown the signal is Lorentzian with its center at ~ 700 kHz. The corresponding experimental signal is shown in Fig. 4(b). It was obtained by scanning the modulation frequency and recording the amplitude of the AMOR. The comparison shows that there is nearly perfect agreement between experiment and simulations. A small discrepancy between positions of the resonances is an artifact originating from simulations. In the transient analysis resonant circuit response depends on the simulation step. In practice, the simulated resonant frequency of the system is lower than the theoretical value. This problem is particularly important for circuits with a high Q factor such as considered in our system.

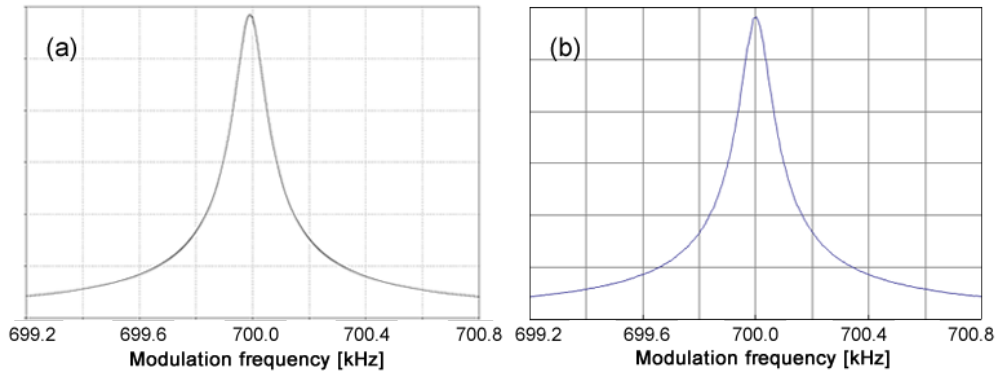


Figure 4. Amplitude of the AMOR signal as a function of the modulation frequency for a longitudinal magnetic field of 50 μT : (a) Simulated electric signal generated with LTspice in the corresponding RLC

circuit, (b) Experimental recording. The signal was measured in the pump-probe arrangement with the balanced polarimeter, which, as shown in Table 1, most accurately corresponds to the actual rotation of the polarization plane generated by atoms.

3.3 Different detection schemes in self-oscillation mode

3.3.1 Modulated pump, unmodulated probe, balanced polarimeter

Successful verification of the electronic model allowed us to proceed to investigation of the AMOR magnetometer in the self-oscillating mode. First, the simulations of the magnetometer in the pump-probe arrangement with the balanced polarimeter were performed. Figure 5 shows diagram of the corresponding electronic equivalent of the detection system. Compared to the case in Sec. 3.2, a small amount of white noise was introduced into B1 current source. Such noise is required in order to initiate the oscillations as the system promotes a particular frequency component of the white-noise spectrum which eventually turns on the oscillations. In order to set the upper limit on the amplitude of oscillations (physical condition), the output signal of the magnetometer is connected back to its input via the automatic gain control (AGC) system (components D1, R1, C1, R2, and Bagc).

The simulation result is shown in Fig. 6. As expected the system starts to oscillate by itself [Fig. 6(a)] reaching the maximum oscillations within ~ 5 ms and oscillating at a frequency strictly determined by the parameters of the RLC circuit

In order to verify whether the system can track the “magnetic-field” changes, at $t=8$ ms the switch S1 connects additional capacitor to our system which detunes its resonance frequency. Modification of the resonance frequency leads to instant change of the oscillation frequency of the system [see inset to Fig. 6(a)].

The theory predicts that the system oscillates sinusoidally (see Table 1). To verify this prediction the FFT of the signal is shown in Fig. 6(b). As seen, only two frequencies are visible on the FFT plot; first corresponds to the oscillations before 8 ms and second after switching the “magnetic field”.

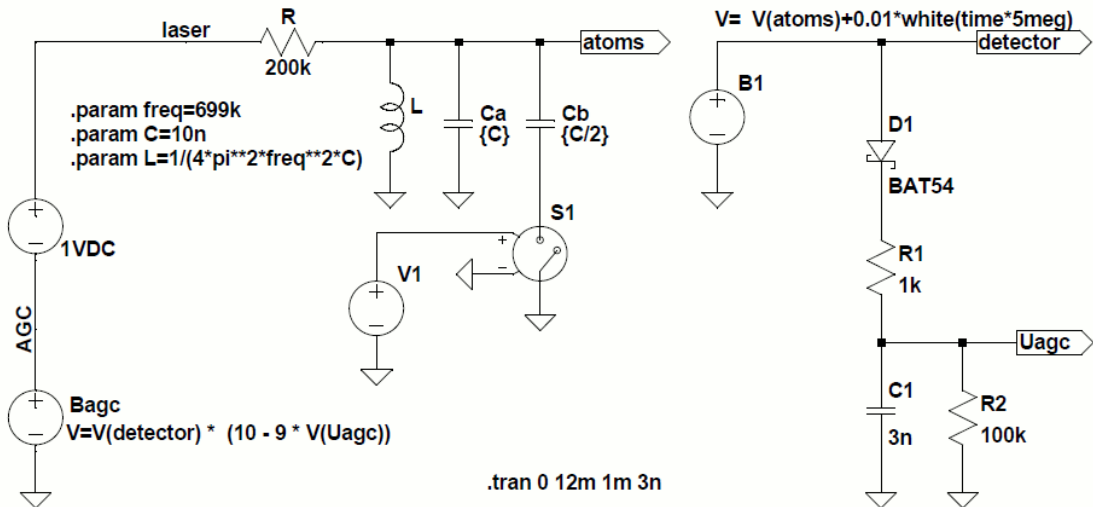


Figure 5. Electronic model of the pump-probe arrangement with the balanced polarimeter.

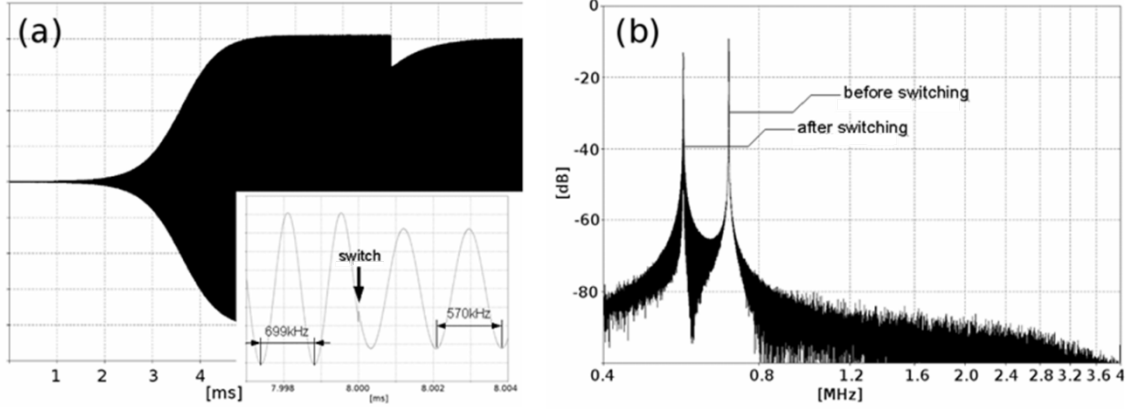


Figure 6. (a) Time-dependent electric signal observed in the system corresponding to the pump-probe arrangement with balanced-polarimeter detection. Inset shows the moment of detuning of the RLC circuit by connection of the additional capacitor and instant response of the system to the change. (b) Fourier transform of the time domain signal with two distinct frequencies corresponding to oscillation before and after connecting the capacitor.

3.3.2 Modulated pump, unmodulated probe, (nearly)-crossed polarizer

Similar simulations as described above were performed for the pump-probe arrangement with (nearly)-crossed polarizer. In the case the circuit diagram remained for the system remains unchanged but the function describing the B1 source is different (see Table 1).

In the pump-probe (nearly)-crossed-polarizer arrangement the signal contains additional, second harmonic of the oscillations. The harmonic results from application of the analyzer tilted by $\sim 90^\circ$. As discussed in Sec. 2.1, in the case of small angle the signal is described by $(\sin\Omega_m t + \Theta)^2$, thus it contains two harmonics for each magnetic fields [see Fig. 7(b)].

Despite the differences between the signals recorded in this and former case, the system easily starts up and oscillates at the resonance frequency very similar as earlier [Fig. 7(a)]. The only noticeable departure from the former case is the starting-up time that is in the present case roughly 4 times longer than that in the former case. It is also demonstrated that a change in the resonance frequency of the RLC circuit leads to instant modification of the oscillation frequency [inset to Fig. 7(a)].

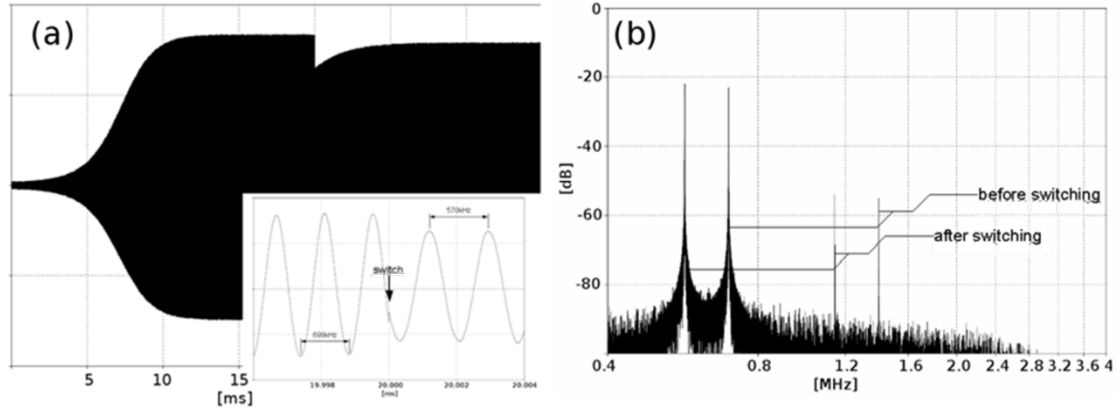


Figure 7. (a) Time-dependent signal recorded in pump-probe arrangement with (nearly)-crossed polarizer. After an initial starting-up time of about 20 ms the oscillation reaches its maximum. The system also instantly responds to the change of the RLC circuit resonance frequency (inset). (b) Fourier transform of the signal with clearly visible second harmonics of the modulation frequency absent in the former case.

3.3.3 Single-beam arrangement with balanced polarimeter

In the magnetometer configuration with a single light beam and the balanced-polarimeter detection the time-dependent electric signal significantly deviates from a pure sine function [Fig. 8(a)]. This distortion is caused by multiplication of the stimulating signal by the response of the medium; after many cycles of the signal within the system a dynamic equilibrium is obtained. The complex character of the recorded signal is best visible on the FFT of the signal where many frequencies are observed before and after detuning the system. Regardless of the complexity of the signal, the oscillations may built up from white noise spontaneously and the self-oscillation regime is achieved [Fig. 8(a)]. It was also demonstrated that the system instantly responses to the change of the RLC resonance frequency (inset), thus the AMOR magnetometer follows magnetic-field changes with no delay.

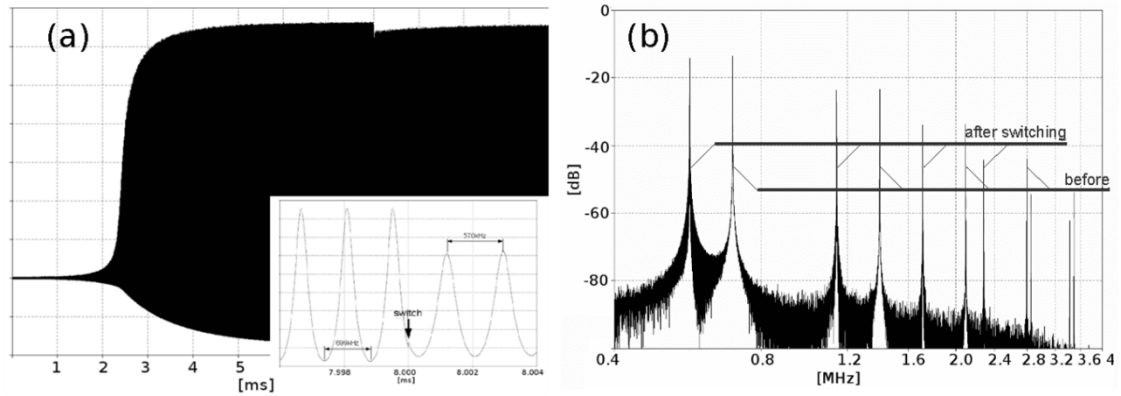


Figure 8. (a) Time-dependent signal recorded in the electronic circuit corresponding to the single-beam arrangement with a balance polarimeter. The signal strongly deviates from the sine function, which

did not prevent the system from entering into self-oscillations and instantly respond to the change of the “magnetic field” (inset). (b) FFT of the recorded spectrum with a number of harmonics corresponding to oscillations before and after changing the RLC circuit’s parameters.

3.3.4 Single beam with (nearly)-crossed polarizer

Due to experimental simplicity (a single light source and one detector) the arrangement exploiting a single light beam and (nearly)-crossed polarizer is appealing for practical applications. Unfortunately, in this configuration the complexity of the signal is the highest which implies that the signal processing is the most challenging among all four discussed cases.

The diagram of the simulated circuit is presented in Fig. 9. As shown, it significantly differs from the circuits used in the former cases. For instance, an additional voltage generator V_{start} , control switches (S2, S3) and voltage sources (V2, V3) are used in the circuit. Initial simulations demonstrated that in the arrangement no oscillations spontaneously rose from the noise. Thus, in order to generate oscillations in the system, the starting generator was needed. The generator is connected to the system for a certain period of time at the beginning of the simulations. Its frequency needs to be carefully adjusted prior the simulations to fulfill the resonance condition of the RLC circuit to start up the system. After achieving given amplitude of the oscillations, the generator is disconnected by the switches S2 and S3 that close a feedback loop in order to achieve self-oscillations.

It is worth noting that in the considered case the system was most efficiently excited with the generator frequency (699.99 kHz) slightly lower than the resonance frequency of the RLC circuit (700 kHz). The difference is once again an artifact of simulations rather than real effect (see discussion in Sec. 3.2).

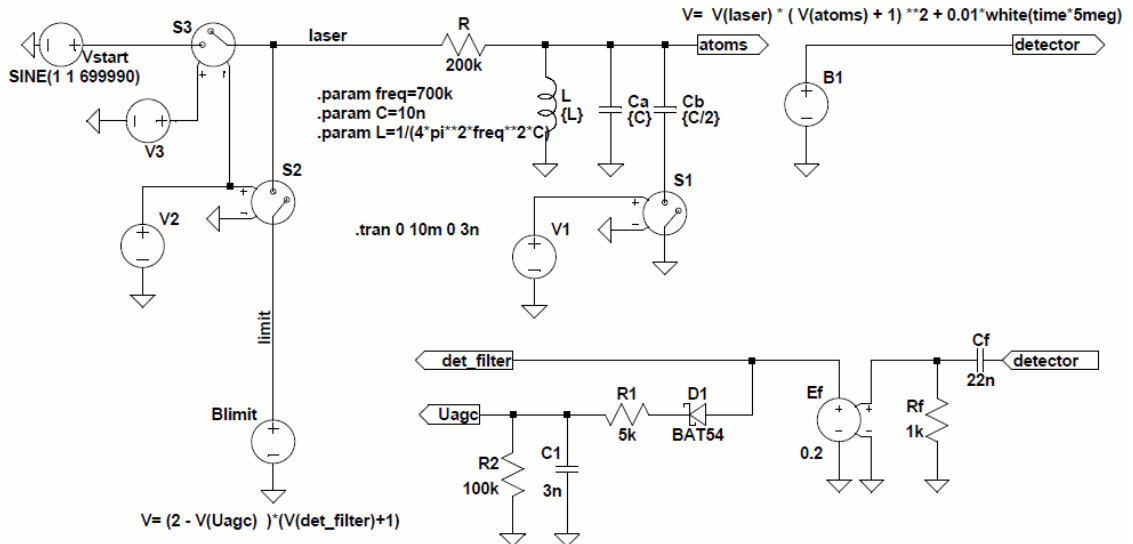


Figure 9. Electronic model and simulation parameters of the single-beam magnetometer with (nearly)-crossed polarizer. An additional voltage generator V_{start} was added to the system in order to start up the oscillations. Switches S2 and S3 start the system in the self-oscillation.

In this arrangement a high-pass filter Rf-Cf is applied to prevent propagation of DC voltage in the feedback loop. The function modeling AGC was also modified to ensure continuous oscillation. Attention was paid to prevent voltage representing the intensity of the laser light going negative.

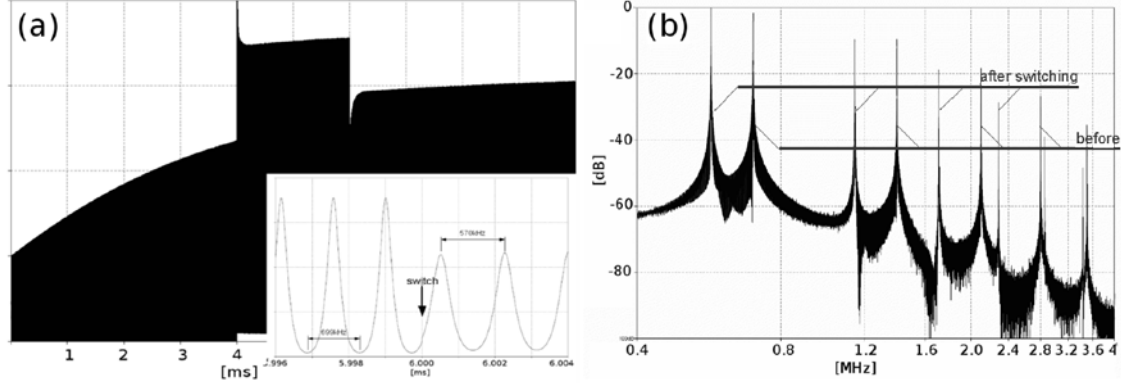


Figure 10. (a) Time-dependent signal recorded in a system corresponding to single-beam (nearly)-crossed polarized magnetometric arrangement. After initial part when the oscillations are excited by external generator, the system was switched into self-oscillation at $t=4$ ms. The system oscillates until the resonance frequency of the RLC was changed ($t=6$ ms) and oscillations at different frequency with slightly lower amplitude were observed (inset). (b) FFT spectrum of the signal with a number of frequency appearing in the signal due to application of single beam and (nearly)-crossed polarizer.

The simulation results are shown in Fig. 10. For the first 4 ms system is driven by the starting generator V_{start} . Strong oscillations right at the start of the simulations are caused by the modulation of light recorded by the detector. The following increase is related to the response of the system to the stimulus. After 4 ms, the feedback loop was closed and the system kept oscillating. The amplitude of the oscillations slightly varied in time but was finally stabilized with AGC circuit. After another 2 ms ($t=6$ ms) a capacitor C_b was connected to RLC system simulating the change in the magnetic field in a real magnetometer. The system immediately responded to the change which demonstrated its potential in tracking the magnetic field. The AGC circuit maintained continuous oscillations. Amplitude of these oscillations depends somewhat on the frequency which is a consequence of the simple function implementing AGC.

4. Experimental results

In order to experimentally verify the predictions of the simulations and confront them with experimental results, the AMOR magnetometer with a single light beam and balanced polarimeter was set up in the self-oscillation mode. The setup was described in details in Ref. [6], here we just briefly review its most important features. It consists of a diode laser emitting light tuned and stabilized to the $F=2 \rightarrow F'=1$ transition in ^{87}Rb (795 nm), acousto-optical modulator (AOM) applied for modulation of light intensity, balanced polarimeter consisting of a crystal Wollaston polarizer and two photodiodes monitoring two channels of the polarizer, and

the paraffin-coated glass cell filled with rubidium vapor enclosed inside a 3-layer mu-metal shield with precisely controlled magnetic field inside. The difference signal of two polarimeter photodiodes is amplified, phase shifted, and introduced into the modulation input of AOM.

Measured signals are shown in Fig. 11. For the sake of convenience the magnetic field was scanned within a range from 1.5 to 2.0 μT which corresponds to the AMOR signal of about 25 kHz. As shown in Fig. 11(a), the signal is periodic with clearly visible second harmonic component of the fundamental frequency. The signal slightly deviates from the one shown in Sec. 3.3.3 but it was experimentally verified that the difference originates from a phase delay present in our system; an appropriate adjustment of the phase delay in our feedback loop resulted in a good agreement between simulations and experimental results.

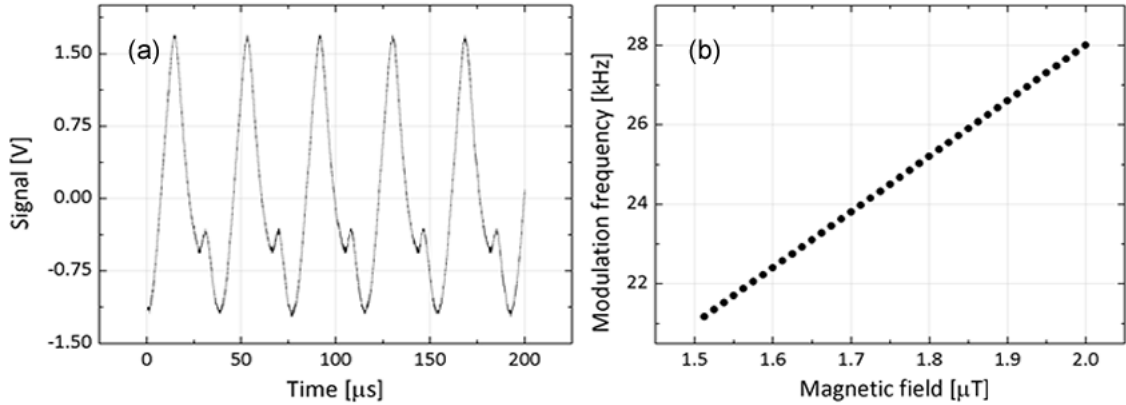


Figure 11. (a) Time-dependent signal recorded in the AMOR magnetometer in single-beam arrangement with balanced polarimeter. The signal is a harmonic oscillation with clearly visible two components of the modulation. (b) The tracking signal recorded in the self-oscillating regime.

Figure 11(b) presents the magnetometer tracking signal. As shown, the modulation frequency strictly followed the magnetic field without any external control. It proves that the magnetometer is operated in self-oscillating mode and predictions of our electronic model are valid.

5. Conclusions

We designed the electronic model of the optical magnetometer based on amplitude-modulated nonlinear magneto-optical rotation (AMOR). The model reproduces the effect well, which was proven by comparison of the simulations with the experimental results, obtained in the passive mode of the magnetometer. Four different electronic circuits were designed in order to simulate four different configurations of the detection system in the AMOR magnetometer. In particular, we investigated all four configurations for operation in the self-oscillating. We proved that any configuration leads to the self-oscillating magnetometer. We set up the magnetometer in the single-beam, balanced polarimeter configuration and demonstrated the possibility of tracking magnetic field. Operation of the magnetometer in the self-oscillating regime opens a possibility for its practical application, in particular, for magnetocardiography. Such application is currently under development.

Acknowledgments

The authors would like to express their gratitude to Mr. P. Wcislo for stimulating discussions. S.P. is a scholar of the Kosciuszko Foundation.

References

- [1] W. Andra and H. Nowak, *Magnetism in Medicine*, Wiley – VCH, New York, 1998.
- [2] D. Budker and M. V. Romalis, *Optical magnetometry*, Nature Phys. 3 (2007) 234.
- [3] P. Wcislo, S. Pustelny, P. Wlodaczyk, and W. Gawlik, *Mapping of magnetic field generated by human heart* – in preparation.
- [4] W. Gawlik and S. Pustelny, *Nonlinear Faraday Effect and its Applications in New trends in quantum coherence and nonlinear optics* (ed. R. Drampyan), pp 45-82, Nova Science Publishers, New York, 2009.
- [5] W. Gawlik, L. Krzemien, S. Pustelny, D. Sangla, J. Zachorowski, M. Graf, A. Sushkov, and D. Budker, *Nonlinear Magneto-Optical Rotation with Amplitude-Modulated Light*, Appl. Phys. Lett. 88 (2006) 131108.
- [6] S. Pustelny, A. Wojciechowski, M. Gring, M. Kotyrba, J. Zachorowski, W. Gawlik, *Magnetometry Based on Nonlinear Magneto-Optical Rotation with Amplitude-Modulated Light*, J. Appl. Phys. 103 (2008) 063108.
- [7] A. L. Bloom, *Principle of Operation of the Rubidium Vapor Magnetometer*, Appl. Opt. 1 (1962) 61.